BIODIVERSITAS
Volume 24, Number 12, December 2023
Pages: 6743-6752

ISSN: 1412-033X
E-ISSN: 2085-4722
DOI: 10.13057/biodiv/d241237

Spatial distribution of paddy field's heavy metals diversity contamination in Samarinda using remote sensing imagery

NURUL PUSPITA PALUPI[1,2,♥], ESTI HANDAYANI HARDI[1], FAHRUNSYAH[2], DWI ERMAWATI RAHAYU[3], RUDY AGUNG NUGROHO[4], SURYA DARMA[2], SURIA DARMA IDRIS[2]

[1]Doctoral Program of Environmental Science, Universitas Mulawarman. Jl. Sambaliung A35 Building, Samarinda 75119, East Kalimantan, Indonesia
[2]Department of Agroecotechnology, Faculty of Agriculture, Universitas Mulawarman. Jl. Paser Balengkong, Samarinda 75243, East Kalimantan, Indonesia. Tel.: +62-541-2083337, ♥email: npuspitapalupi@faperta.unmul.ac.id
[3]Department of Environment Technology, Faculty of Technology, Universitas Mulawarman. Jl. Sambaliung, Samarinda 75242, East Kalimantan, Indonesia
[4]Department of Biology, Head of Microbiological Laboratory, Faculty of Mathematics and Sciences, Universitas Mulawarman. Jl. Barongtongkok, Samarinda 75242, East Kalimantan, Indonesia

Manuscript received: 28 September 2023. Revision accepted: 26 December 2023.

Abstract. *Palupi NP, Hardi EH, Fahrunsyah, Rahayu DE, Nugroho RA, Darma S, Idris SD. 2023. Spatial distribution of paddy field's heavy metals diversity contamination in Samarinda using remote sensing imagery. Biodiversitas 24: 6743-6752.* The adverse effects of heavy metal contamination on rice fields posing a significant threat to food safety. This study, conducted from May to July 2023 in Samarinda East Kalimantan, Indonesia, aims to determine the distribution of active rice fields and heavy metal contamination through Kriging's interpolation method. Aerial photographic interpretations, facilitated by ArcGIS 10.4, were performed with 144 sample points within 4 Districts. The content of heavy metals was assessed by Atomic Absorption Spectroscopy at specific wavelengths: 248.3 nm for Fe, 228.8 nm for Pb, 283.3 nm for Cd, 357.9 nm for Cr, 279.5 nm for Mn, 213.9 nm for Zn, and 324.7 nm for Cu, following guidelines of SNI 8910:2021. The research showed that existing rice fields were concentrated in North Samarinda District (380,416 ha), Loa Janan Ilir District (210,133 ha), Sambutan District (404,682 ha), and Palaran District (188,617 ha) with Fe content ranged from 4.976,45 ppm to 16.800,485 ppm, exceeding the critical Fe limit in soil of 500 ppm set by SNI. Mn content ranged from 22.65 ppm to 564.88 ppm, surpassing the critical soil threshold of 0.15 ppm for Mn according to SNI. Cu content varied from 3.32 ppm to 121.75 ppm, exceeding critical Cu limit of 0.04 ppm. Zn content ranged from 8.61 ppm to 223.12 ppm, surpassing the critical limit of Zn's pollution in the soil (0.06 ppm). Pb content ranged from 10.72 ppm to 32,84 ppm, categorized as intermediate compared to the threshold of 0.07 ppm for Pb in soil. Cd content ranged from 0.04 ppm to 0.739 ppm, exceeding the critical limit of 0.01 ppm set by SNI. Cr content was detected to be less than 0.032 ppm, falling into a very low category, with the critical limit for Cr content in soil set at 0.5 ppm according to SNI.

Keywords: Contamination, heavy metals, kriging, mapping accuracy, paddy field

INTRODUCTION

Soil plays a fundamental role in ensuring food safety, and the adverse effects of contaminants such as heavy metals on plant quality pose a threat to human health (Qin et al. 2021). Beyond impacting plant health, accumulating evidence suggests a correlation between heavy metal exposure and various diseases in humans (Wang et al. 2020). To mitigate health risks, effective measures are necessary to reduce the accumulation of metals, especially Cu and Zn, in rice fields, preventing their translocation from soil to the edible parts of plants (Abuzaid and Bassouny 2020). The availability ratio of metals in soil is intricately linked to pH, organic matter, and soil microbial activity (Jiang et al. 2021).

Study by Akter et al. (2022) indicates that pesticides contribute to the presence of heavy metals in rice fields, which contain heavy metals such as As, Cu, Zn, Mn, Hg, Pb in high amounts. reported that pesticides contain As 0.8-60 ppm, Cu 4-56 ppm, Hg 0.6-42 ppm, Mn 1-17 ppm, Pb 11-60 ppm, and Zn 1-30 ppm, which is one of the sources contamination of these elements alongside the consequences of the overuse of pesticides and chemical fertilizers (Hembrom et al. 2020). The excessive use of agrochemicals not only deteriorates soil and water quality (Srivastav 2020) but also poses high vulnerabilities, mainly impacting socioeconomic development, negatively affecting food safety, and increasing carcinogenic risks (Jiang et al. 2020). The contamination of heavy metals in rice fields is attributed to various factors, including wastewater irrigation, sewage sludge application, livestock manure, mining (Qin et al. 2021), and mineral rock plating (Bashir et al. 2020). Consequently, heavy metals and metalloids, such as Cd^{2+}, Zn^{2+}, Cu^{2+}, Cr^{2+}, Ni^{2+}, Fe^{2+}, and Fe^{3+}, accumulate in rice components (root, straw, chaff, and grain) at different levels (Sharma et al. 2021).

Li et al. (2022a) emphasize that agricultural land contributes to heavy metal presence in the soil, and effective government prevention and control policies can significantly reduce heavy metal smelting, ensuring the safety of all agricultural products for consumption. Mapping through remote sensing or aerial photography involves collecting image data, followed by image correction and digitization into a line map. Remote sensing image interpretation, categorized as visual or digital, aims to identify objects within the images (Knuth et al. 2023).

Visual interpretation is conducted on a computer monitor, focusing on the visual examination of the Earth's surface depicted in images to identify objects and assess their significance. The elements of image interpretation include hue or color, size, shape, texture, pattern, shadow height, site, and association (Li et al. 2022b). Identification of the presence of heavy metals in paddy soil needs to be done precisely, this can be done through a soil survey by collecting chemical data on heavy metal content in the laboratory and then the results of the analysis are mapped by grouping soils of the same and almost identical nature into certain soil map units. The research area is based on rice fields in Samarinda City which are suspected of experiencing pollution due to surrounding activities.

Determining existing rice fields in an area is important for calculating the need for rice for the people of an area so that the shrinkage and contamination of rice fields can be seen as a basis for local governments to make efforts to reduce and prevent contamination. Based on this argument, it is very important research to reach the distribution of heavy metal contaminants like Fe, Mn, Cu, Cr, Cd, Zn in existing rice fields in Samarinda.

MATERIALS AND METHODS

Study area

The study was conducted in Samarinda, East Kalimantan, Indonesia, from March to July 2023, situated geographically at coordinates 116° 15' 36"-117° 24' 16" BT and 0° 21' 18" - 1° 09' 16" LS. The processing and analysis of spatial data were conducted at the Cartography Laboratory and Geographic Information System of the Faculty of Agriculture at Universitas Mulawarman, utilizing both primary and secondary data sources.

Primary data were derived from high-resolution satellite imagery spot 7th on March 7th 2023 with a resolution of 15 meters per pixel. Secondary data encompassed various sources, including administrative maps of Samarinda City, publications, studies, and other relevant materials such as administrative maps, land-use maps, RTRW maps, topographic maps, and maps depicting Samarinda City land systems. These secondary data were collected through organizational observations and sourced from entities such as *Badan Perencanaan Pembangunan Daerah*-BAPPEDA (Development Planning Agency at Sub-National Level), Samarinda City, the Samarinda City Central Statistics Agency, the Samarinda City Agriculture Office, and the Samarinda City Public Works Office.

Procedures

Processing, analysis and layout creation

The ArcGIS 10.4 was employed for data pre-processing, systematically correcting radiometric distortions to mitigate atmospheric interferences as outlined by Tmušić et al. (2020). Subsequent steps involved image cropping to enhance focus, detail, and optimize data processing, ensuring the creation of a representative, uninterrupted image. The image was further positioned to align with real-world map coordinates, aiming to eradicate distortions caused by Earth's rotation, satellite motion, and surface curvature, adhering to the methodologies proposed by Knuth et al. (2023). Image editing was conducted to augment the interpretability of data, catering to both digital and manual interpretation.

The interpretation of satellite imagery encompassed analysis of tone, color, shape, texture, pattern, shadow, location, and object associations. This process involved distinct activities including separation, delineation, recognition, and pattern discovery, in accordance with framework of Ha et al. (2020) for comprehending and interpreting satellite image content.

Heavy metals soil sampling

The soil sampling in depth 0-20 cm from surface for determining the distribution of contaminants was done at several random points in existing rice fields in Loa Janan Ilir District, Palaran District, Sambutan District, North Samarinda District. Analysis of Pb^{2+}, Cd^{2+}, Cr^{3+}, Cu^{2+}, Mn^{2+}, and Fe^{3+} contents was conducted at the Agricultural Faculty of Agriculture and Water Resources Laboratory of the Faculty of Fisheries and Marine Sciences of Mulawarman University. The content of heavy metals were determined by measuring the description of soil samples which destroyed by wet ashing method with a mixture of strong acids HNO_3 (65% pa) and $HClO_4$ (60% pa) using Atomic Absorption Spectroscopy (SSA) at wavelengths of 248.3 for Fe, 228.8 nm for Pb, 283.3 nm for Cd, 357.9 nm for Cr, 279.5 nm for Mn, 213.9 nm for Zn, and 324.7 nm for Cu, with reference to SNI 8910:2021 (BSN 2021). After the heavy metal content in the soil were known, the Kriging method was used to estimate the value of soil content. This method assumes that the distance and orientation between data samples show important spatial correlations in the interpolation results.

Data analysis

The results were categorized based on evaluation criteria established by the Balittanah Bogor (2005) and the Ministry of State for Population and Environment of Indonesia, and Dalhousie University Canada (1992). Subsequently, these categorized results were organized into maps utilizing the ArcGIS 10.4. This mapping process allowed for a visual representation of the distribution of analyzed parameters, facilitating a comprehensive understanding of the soil analysis outcomes.

RESULTS AND DISCUSSION

Paddy field distribution in Samarinda

Physiographically, Samarinda City is predominantly characterized by fault areas, encompassing 41.12% of its total area, equivalent to 295.26 km^2. This is followed by a plain area covering 10,524 km^2, accounting for 14.66% of Samarinda City's total area. In terms of topography, the city mainly consists of relatively flat land, with approximately 27.39% having a slope of less than 2% and 24.47% at a slope ranging from 2-15% (Figure 1).

Regarding soil depth classification, the majority of Samarinda's area exhibits soil depths exceeding 90 cm, encompassing 39,833 hectares or 55.48% of the total area (Table 1). This area falls within the Tropika Humida climate type and features soil types classified as reactive to acidity, categorized under Soil Taxonomic USDA classifications such as Ultisol, Entisol, and Histosol. Alternatively, according to the Bogor Land Research Institute, soil types consist of Podsolic, Alluvial, and Organosol. Podsolic Land (Ultisol) comprises approximately 57.57% of Samarinda's land area (Figure 2), with abundant water supplies primarily sourced from heavy rainfall. Spatially, the active rice fields in 2023 cover 1,734.26 ha out of the total land area of 71,726.59 ha in Samarinda (Figure 3). Details of the active rice fields per subdistrict are outlined in Table 2, revealing a 52% reduction in active rice fields since 2002 attributed to changes in land function.

The distribution of heavy metals in rice fields across four sub-districts in Samarinda-Loa Janan Ilir (Figure 4), North Samarinda District (Figure 5), Sambutan District (Figure 6), and Palaran District (Figure 7)-revealed noteworthy findings. The concentration of Fe in rice fields ranged from 4,976.45 ppm to 16,800.485 ppm, surpassing the critical limit of 500 ppm according to SNI. Elevated Fe levels in soil pose a significant challenge to rice production, leading to reduced yields and potential crop failure (Rakotoson et al. 2022; Dossou-Yovo et al. 2023). Studies (Ahmed et al. 2023) suggest that Fe toxicity hinders proper growth, resulting in stunted development and low production. High Fe content in soil negatively impacts the availability of essential elements (Briat et al. 2020), and various methods, such as using Si (dos Santos et al. 2020), have been explored to mitigate dissolved Fe in soil. Fe distribution by the Kriging method were presented in Figure 8.

The Mn content in rice fields ranged from 22.65 ppm to 564.88 ppm, exceeding the critical soil threshold of 0.15 ppm according to SNI and its distribution were presented in Figure 9. Mn toxicity is influenced by pH, organic matter, and soil moisture, with concentrations exceeding 200 ppm posing a risk (Wu et al. 2020). Soil with a pH below 5.5 enhances Mn solubility, and Mn4+ reduction to Mn2+ in poorly drained soil conditions further increases solubility (Zahoransky et al. 2022). Different metals affect plants differently, with their toxicity varying based on concentrations and plant types. Soil physics-chemical parameters such as pH, cation exchange capacity (KTK), texture, and organic matter influence metal absorption (Daulta et al. 2023).

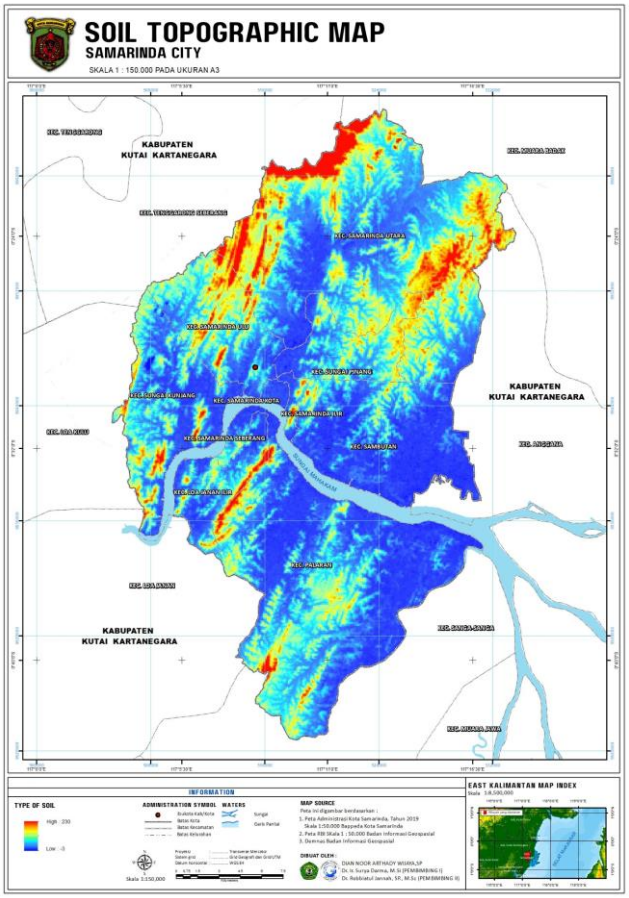

Figure 1. Soil topographic map

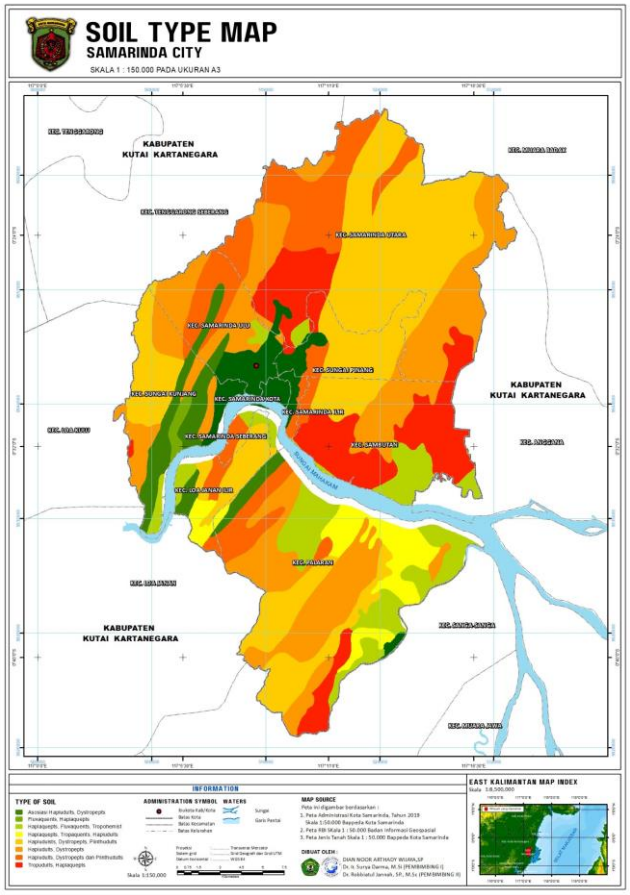

Figure 2. Soil type map

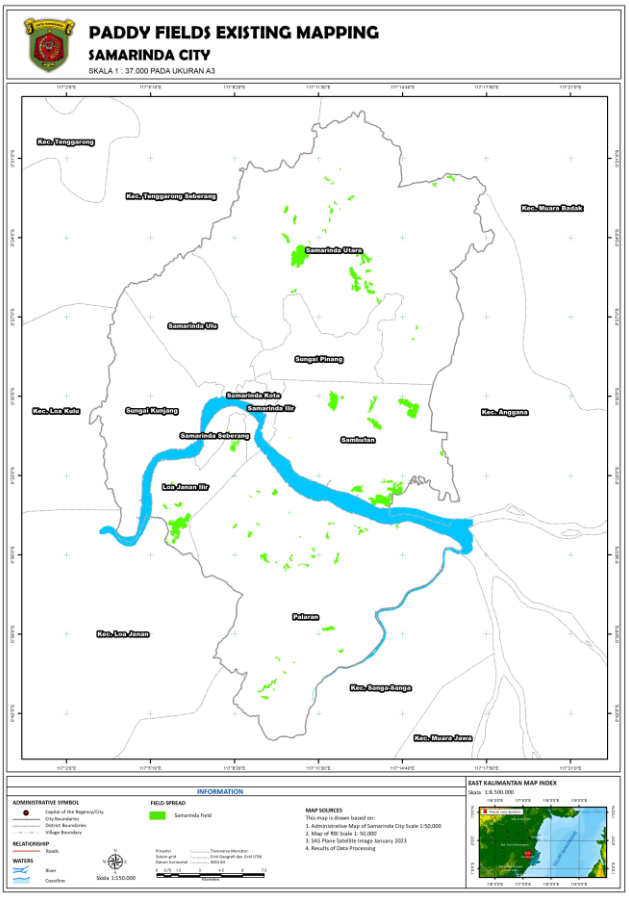

Figure 3. Spatial map of existing paddy fields in Samarinda, 2023

Mn has antagonistic interactions with Fe, impacting their concentrations in plant tissue (Zheng et al. 2020), and maintaining a Fe:Mn ratio within the range of 1.5 and 2.5 is crucial (Cakmak et al. 2023). Addressing Mn poisoning in acid soil involves raising pH above 6.5 (Palansooriya et al. 2020). The Cu content in rice fields ranged from 3.32 ppm to 121.75 ppm, surpassing the critical Cu limit of 0.04 ppm (Bedoya-Perales et al. 2023). Cu pollution sources include air and water, impacting soil (Qin et al. 2021). The magnitude of heavy metal content in plant media influences metal absorption by plants (Diaconu et al. 2020), and elevated Cu levels above permissible thresholds can lead to diseases (Mitra et al. 2022). Soil characteristics such as cation exchange capacity and total organic carbon are negatively correlated with extractable Cu content (Zhang et al. 2020).

Zn content in rice fields ranged from 8.61 ppm to 223.12 ppm, exceeding the critical limit of Zn pollution in soil, which is below 0.06 ppm (Oprčkal et al. 2020). Clay content influences Zn levels, with higher clay fractions leading to greater clay colloid absorption of Zn (Moreno-Lora and Delgado 2020). Additionally, soil pH affects Zn content, decreasing as soil pH increases (Laurent et al. 2020). Vegetation activities contribute to nutrient transfer between soil layers (Jaskulak et al. 2020), and Zn is easier for rice to accumulate compared to other plants. Hazard quotient (HQ) calculations suggest potential non-carcinogenic and carcinogenic health risks associated with rice consumption (Wang et al. 2023). Pb content in rice fields ranged from 10.72 ppm to 32.84 ppm, categorized as intermediate based on the threshold of 0.07 ppm in soil (Steliga and Kluk 2020). pH and soil texture influence Pb content (Stefanowicz et al. 2020), with acidic soil increasing metal availability. Clay fractions, particularly in high amounts, enhance clay colloid absorption of Pb (Otunola and Ololade 2020).

Table 1. Slope class and slope area of Samarinda City

Items	Coverage (Ha)	Percentage (%)
Slope	**71800.00**	**100.00**
<2	19663.19	27.39
2-15	18290.88	24.47
15-25	10630.59	14.81
25-40	11248.92	15.67
>40	9348.90	13.02
Waters	2617.52	3.65
Depth Class	**71800.00**	**100.00**
<30	-	-
30-60	11544.13	16.08
60-90	17805.32	24.80
>90	39833.03	55.48

Notes: Central Bureau of Statistics, 2023 (Source)

Table 2. Existing paddy field area per District (2002-2023)

District	Area (ha)	Paddy fields area (ha)		
		2002	2011	2023
Samarinda Utara	22,422.92	1,121.48	842.26	380.416
Sungai Pinang	3,487.17	51.79	10.40	-
Sungai Kunjang	7,187.75	71.55	21.33	5.67
Samarinda Seberang	1,035.61	12.35	6.81	-
Loa Janan Ilir	3,039.82	265.97	325.15	210.133
Palaran	19,679.48	1,208.29	479.66	188.617
Sambutan	8,970.53	551.02	521.67	404.682
Samarinda Kota	356.02	-	-	-
Samarinda Ilir	511.05	-	-	-
Samarinda Ulu	5,036.24	1.32	-	-
Total	71,726.59	3,283.78	2,207.28	1,189.518

Notes: Spatial Analysis Results, 2023 (Source)

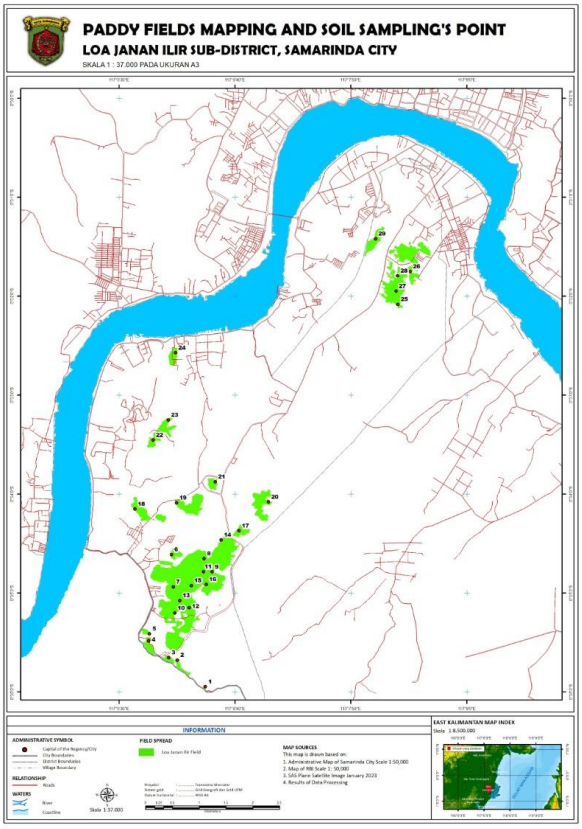

Point	X	Y	Fe	Mn	Cu	Zn	Pb	Cd	Cr
			ppm						
1	511810,797	9933778,338	9807,929	250,010	17,452	25,340	34,128	0,278	<0,032
2	511288,693	9934274,869	9453,818	278,410	16,994	24,937	34,768	0,336	<0,032
3	511126,620	9934319,624	9454,617	252,890	19,866	26,672	35,506	0,293	<0,032
4	510751,579	9934628,800	9715,520	252,320	18,461	26,250	36,345	0,315	<0,032
5	510766,384	9934762,063	7966,033	155,810	13,728	42,222	11,950	0,140	<0,032
6	511177,789	9936237,121	9717,097	254,320	21,987	25,790	36,992	0,434	<0,032
7	511211,589	9935637,716	11076,025	366,583	17,065	52,837	16,157	0,354	<0,032
8	511786,167	9936161,838	10499,411	338,396	20,063	70,872	15,203	0,349	<0,032
9	511934,855	9935917,219	13779,120	533,198	40,834	122,581	26,311	0,603	<0,032
10	511241,226	9935150,186	11621,950	368,720	40,311	126,567	25,725	0,618	<0,032
11	511778,059	9935918,311	13682,528	559,062	37,332	125,983	26,668	0,629	<0,032
12	511508,430	9935252,152	12623,336	560,914	38,925	125,366	25,546	0,637	<0,032
13	511334,841	9935381,661	14624,523	551,323	39,546	127,088	27,821	0,641	<0,032
14	512104,698	9936510,618	13812,321	562,567	41,677	126,675	28,934	0,678	<0,032
15	511550,377	9935660,522	13613,373	563,989	40,848	125,860	27,568	0,695	<0,032
16	511826,649	9935684,420	8414,326	564,882	38,739	125,215	27,959	0,600	<0,032
17	512439,285	9936683,243	9815,667	498,651	21,555	26,714	36,884	0,335	<0,032
18	510496,018	9937086,038	9274,504	106,326	17,792	37,291	18,457	0,346	<0,032
19	511271,088	9937200,518	11122,773	57,939	24,196	45,933	12,286	0,399	<0,032
20	512989,671	9937217,480	9818,115	168,312	19,563	36,133	16,051	0,359	<0,032
21	511998,500	9937592,039	9679,329	234,543	21,886	35,492	17,183	0,291	<0,032
22	510837,073	9938368,723	14615,152	375,509	30,548	102,621	21,655	0,600	<0,032
23	511117,533	9938742,897	14459,198	392,108	33,334	75,052	19,523	0,576	<0,032
24	511254,828	9939996,719	12401,003	251,957	38,029	107,740	21,992	0,643	<0,032
25	515405,660	9940895,641	9655,392	273,927	29,734	26,558	34,855	0,446	<0,032
26	515635,391	9941507,588	9980,014	294,323	29,656	25,358	34,018	0,432	<0,032
27	515368,829	9941142,610	8685,929	277,842	21,083	25,775	35,670	0,295	<0,032
28	515398,901	9941428,351	8746,041	239,326	27,339	23,546	38,696	0,338	<0,032
29	514988,071	9942116,854	9687,457	277,763	22,396	27,500	37,004	0,357	<0,032

Figure 4. Distribution of heavy metals contamination in paddy fields in Loa Janan Ilir Sub-district

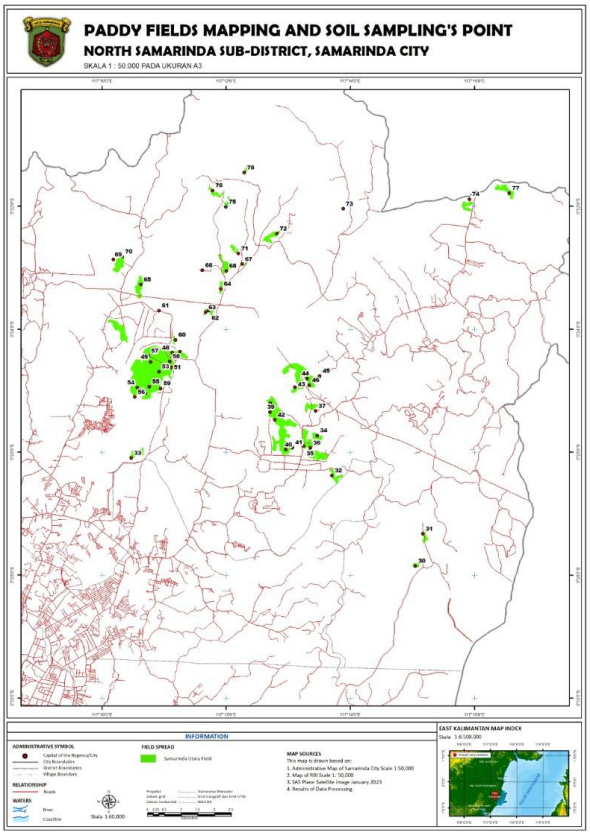

Point	X	Y	Fe	Mn	Cu	Zn	Pb	Cd	Cr
			ppm						
1	527904,426	9948688,244	12290,014	168,920	23,749	71,366	21,965	0,672	<0,032
2	528131,975	9949651,497	13798,266	161,640	21,476	67,088	23,484	0,689	<0,032
3	525417,944	9951398,975	15991,877	119,068	16,660	66,675	18,658	0,673	<0,032
4	519417,470	9951924,581	9097,770	120,972	12,665	65,860	16,004	0,401	<0,032
5	524970,889	9952597,707	13397,438	146,821	36,001	59,909	13,576	0,519	<0,032
6	524571,747	9952284,085	16800,485	149,298	37,433	56,788	14,599	0,577	<0,032
7	524767,148	9952227,653	9672,865	141,684	36,878	56,660	14,576	0,507	<0,032
8	524930,214	9953335,199	6317,766	172,765	38,577	91,537	23,704	0,739	<0,032
9	523579,745	9953566,020	14812,865	210,711	22,935	71,201	18,626	0,686	<0,032
10	523567,065	9953300,093	14549,098	222,033	19,546	71,499	18,679	0,611	<0,032
11	524036,515	9952174,649	14290,233	221,745	27,100	74,321	17,460	0,687	<0,032
12	524234,516	9952239,280	14087,680	218,570	28,433	77,334	17,786	0,676	<0,032
13	523708,568	9953066,222	16149,588	222,745	26,489	76,125	17,100	0,544	<0,032
14	524309,214	9954040,743	14878,647	122,454	28,346	71,558	19,608	0,668	<0,032
15	524676,206	9954304,574	16675,009	114,654	21,656	75,358	17,044	0,627	<0,032
16	525051,602	9954383,594	12397,729	148,624	26,893	75,780	17,997	0,670	<0,032
17	524733,993	9954108,854	15676,099	171,469	24,344	72,234	23,843	0,774	<0,032
18	520875,227	9955111,435	9987,730	193,956	17,155	48,986	12,454	0,502	<0,032
19	520641,219	9955079,117	8719,008	206,025	81,082	40,876	11,054	0,608	<0,032
20	519995,224	9954798,906	14190,346	168,920	24,027	70,389	21,010	0,606	<0,032
21	519835,155	9953860,936	14792,570	161,640	22,451	77,088	22,446	0,680	<0,032
22	520603,427	9954639,727	8977,045	119,068	15,652	56,679	17,659	0,588	<0,032
23	520402,949	9954700,551	9090,496	120,972	12,628	55,882	15,010	0,150	<0,032
24	520250,914	9954509,062	11387,468	146,821	36,760	57,909	13,576	0,609	<0,032
25	519598,710	9954029,347	7890,976	149,287	37,196	56,714	14,599	0,522	<0,032
26	519956,322	9954060,379	7672,911	141,787	36,026	57,000	13,576	0,512	<0,032
27	519526,366	9953754,038	13312,832	142,765	38,640	91,537	26,704	0,765	<0,032
28	519925,077	9954981,829	12912,039	140,711	22,853	71,200	18,626	0,675	<0,032
29	520566,022	9954816,161	14129,122	122,560	19,988	71,473	19,010	0,677	<0,032
30	520294,153	9954006,693	14990,284	121,766	27,987	74,345	18,453	0,681	<0,032
31	520743,136	9955464,566	15187,099	118,346	28,356	77,338	18,736	0,657	<0,032
32	520247,568	9956340,938	15499,581	122,745	26,087	76,100	17,046	0,677	<0,032
33	521735,072	9956349,250	14878,647	120,876	28,388	71,556	19,645	0,682	<0,032
34	521640,639	9956291,444	15675,915	119,655	21,876	75,300	17,457	0,570	<0,032
35	522101,063	9956986,395	12397,725	118,624	26,443	75,778	17,900	0,670	<0,032
36	519709,941	9957121,798	15648,356	171,469	24,599	72,234	23,843	0,754	<0,032
37	521540,893	9957547,276	8591,469	93,956	17,155	48,986	12,454	0,511	<0,032
38	522736,296	9957742,116	8609,454	88,546	18,736	40,473	11,054	0,624	<0,032
39	522261,520	9957527,969	14812,031	110,711	22,819	71,200	18,626	0,696	<0,032
40	518884,618	9957867,104	8773,436	122,432	19,559	71,492	18,010	0,681	<0,032
41	519147,711	9957959,650	8990,285	121,346	27,671	74,365	19,452	0,681	<0,032
42	522621,037	9958052,407	11837,988	118,679	28,624	74,533	18,786	0,658	<0,032
43	523768,224	9958645,196	12479,358	122,999	26,479	76,121	17,089	0,677	<0,032
44	525747,013	9959392,544	9878,666	120,445	28,654	71,600	19,689	0,682	<0,032
45	529519,825	9959679,273	10675,968	119,099	21,874	75,357	17,044	0,565	<0,032
46	522244,401	9959448,886	11397,468	118,456	26,034	75,775	17,457	0,681	<0,032
47	521849,248	9959936,145	13648,356	171,469	24,779	72,234	23,843	0,875	<0,032
48	530711,770	9959858,767	12591,732	93,956	7,122	48,986	12,454	0,491	<0,032
49	522791,625	9960474,160	9619,435	88,568	8,778	40,483	11,054	0,458	<0,032

Figure 5. Distribution of heavy metals contamination in paddy fields in North Samarinda Sub-district

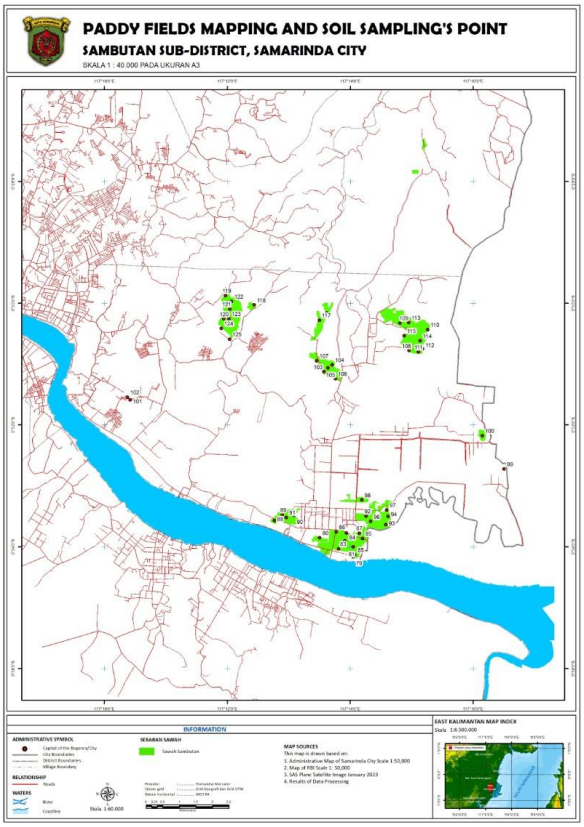

Point	X	Y	Fe	Mn	Cu	Zn	Pb	Cd	Cr
			ppm						
1	519704,148	9926104,102	14830,666	219,631	20,563	55,054	15,983	0,050	<0,032
2	519388,464	9926138,135	5722,043	223,343	12,395	46,984	14,609	0,045	<0,032
3	519575,057	9926162,057	5613,678	219,561	13,821	49,835	14,994	0,047	<0,032
4	518606,490	9926286,896	13986,432	218,497	12,568	53,745	14,309	0,044	<0,032
5	523020,357	9927039,593	13772,545	217,022	19,492	42,764	14,841	0,050	<0,032
6	521962,655	9928401,044	8778,127	123,552	11,129	56,782	14,250	0,070	<0,032
7	521661,417	9928572,081	8768,638	117,342	12,786	55,895	14,010	0,069	<0,032
8	518865,791	9932183,805	5603,556	120,560	19,459	58,554	16,787	0,057	<0,032
9	520322,810	9932180,189	5492,114	121,642	13,012	55,541	14,885	0,080	<0,032
10	520443,664	9932354,341	4953,287	123,761	14,785	55,774	17,569	0,068	<0,032
11	520404,455	9932824,545	3823,718	117,442	14,676	56,054	14,769	0,073	<0,032
12	520678,066	9932898,741	4687,234	118,627	17,526	55,398	14,699	0,070	<0,032
13	521022,811	9932706,762	5668,331	120,446	13,871	55,895	14,888	0,070	<0,032
14	519204,020	9932805,008	9503,973	267,147	13,336	91,678	17,167	0,103	<0,032
15	520568,142	9933024,033	8977,882	221,870	11,854	77,544	18,544	0,046	<0,032
16	519164,429	9933163,073	8130,037	136,392	11,265	66,504	20,140	0,060	<0,032
17	518223,527	9933250,019	8856,675	120,796	13,631	65,945	19,554	0,096	<0,032
18	522572,229	9933416,072	11050,144	291,575	9,990	63,639	18,121	0,151	<0,032
19	520786,898	9933671,642	9976,457	218,739	9,342	62,643	17,984	0,168	<0,032
20	519521,189	9933571,869	10786,962	188,537	8,138	63,263	15,596	0,180	<0,032
21	522609,077	9933678,598	11013,028	209,677	10,542	82,425	17,055	0,282	<0,032
22	517266,064	9933667,358	15388,038	216,843	15,539	84,634	18,075	0,188	<0,032
23	517464,371	9933448,232	15902,542	213,330	17,357	83,005	17,996	0,107	<0,032
24	521071,348	9933934,702	14308,935	221,673	17,435	82,996	17,495	0,130	<0,032
25	520919,904	9934161,301	14967,564	222,896	13,347	82,564	18,776	0,210	<0,032
26	524292,703	9934846,673	15443,727	216,235	18,434	93,886	17,232	0,105	<0,032
27	524284,987	9934628,263	15644,455	213,780	16,074	92,008	17,775	0,110	<0,032
28	524153,491	9934555,746	15348,346	219,455	19,137	102,856	18,447	0,202	<0,032
29	520035,133	9935036,911	14976,772	223,017	13,339	82,005	17,777	0,105	<0,032
30	516693,173	9934965,325	15683,525	221,787	16,945	112,445	18,229	0,185	<0,032
31	516858,301	9934459,582	15487,888	214,676	121,746	123,775	17,745	0,111	<0,032
32	516888,545	9934822,760	14879,015	217,522	14,128	112,661	18,187	0,114	<0,032
33	521999,234	9934699,145	11611,688	112,590	18,164	141,602	18,738	0,108	<0,032
34	516566,556	9935160,785	8303,741	94,796	22,424	120,777	17,399	0,106	<0,032
35	519637,743	9935250,566	8272,457	52,772	20,870	42,457	15,764	0,105	<0,032
36	521506,564	9935354,909	12177,722	79,392	19,478	124,131	17,560	0,140	<0,032
37	520268,411	9935269,434	12967,495	73,632	16,521	93,634	16,775	0,240	<0,032
38	526117,303	9935616,898	12879,569	74,125	16,688	94,775	17,560	0,190	<0,032
39	519592,002	9935543,452	13793,990	80,344	26,418	100,344	15,007	0,338	<0,032
40	524498,785	9935187,788	14532,880	87,654	15,503	87,601	17,377	0,437	<0,032
41	524154,667	9935152,997	13799,323	91,294	14,234	91,443	15,213	0,410	<0,032
42	526557,725	9935554,346	12463,837	90,346	11,946	90,899	16,336	0,437	<0,032
43	526893,577	9935511,205	12604,554	98,457	14,726	78,458	15,789	0,419	<0,032
44	523935,259	9935751,244	12654,722	90,477	15,280	80,112	15,560	0,410	<0,032
45	515439,093	9935749,567	11312,326	183,526	21,175	77,541	14,530	0,424	<0,032
46	517052,534	9935742,157	9590,810	120,670	23,884	55,383	16,004	0,322	<0,032
47	522103,545	9935907,627	9751,099	42,593	19,442	38,747	17,672	0,228	<0,032
48	522389,064	9935904,032	9976,930	122,380	7,496	59,877	16,385	0,322	<0,032
49	515713,636	9935913,846	9821,860	121,390	5,964	100,635	15,004	0,462	<0,032
50	516112,151	9936556,632	10141,016	257,282	4,995	171,943	14,362	0,571	<0,032
51	519264,099	9936604,019	8547,930	120,154	6,460	117,830	14,006	0,472	<0,032
52	516496,152	9936858,524	9476,746	217,680	12,365	121,313	14,221	0,466	<0,032
53	516661,661	9937170,472	9580,346	214,249	10,297	171,785	14,613	0,460	<0,032
54	516724,631	9937280,939	7769,684	217,831	3,320	222,637	14,070	0,270	<0,032
55	516530,163	9937464,553	6867,450	221,312	3,535	223,119	14,231	0,379	<0,032
56	516591,008	9937758,496	5818,061	213,785	9,653	113,677	14,119	0,377	<0,032
57	516638,270	9937739,119	6204,228	222,637	4,596	113,491	14,301	0,270	<0,032
58	516765,423	9937769,420	6276,420	223,119	12,383	46,255	14,373	0,268	<0,032

Figure 6. Distribution of heavy metals contamination in paddy fields in Sambutan Sub-district

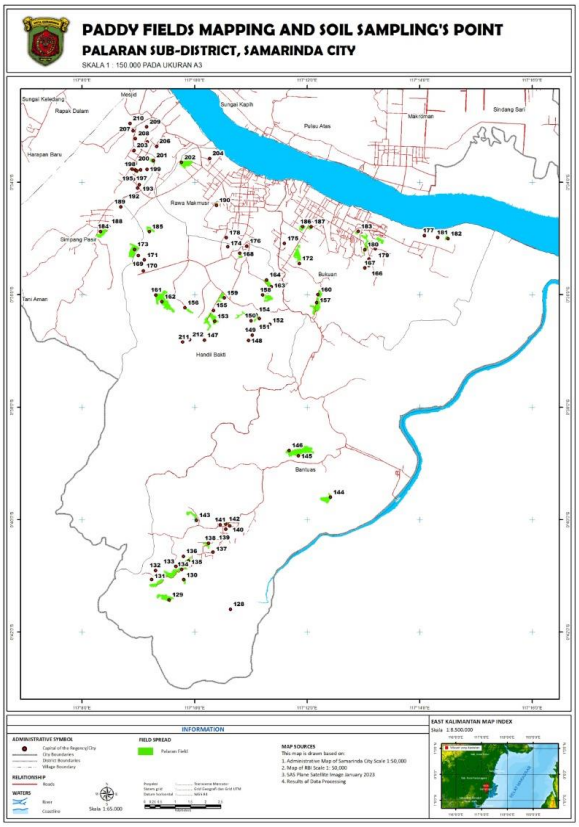

Point	X	Y	Fe	Mn	Cu	Zn	Pb	Cd	Cr
			ppm						
1	516485,867	9937792,717	6357,990	113,677	11,397	40,992	14,006	0,271	<0,032
2	516977,439	9937787,143	6190,388	113,491	15,812	39,856	14,117	0,287	<0,032
3	516597,115	9937970,298	6657,940	46,255	12,157	44,789	14,443	0,267	<0,032
4	517186,586	9938076,778	6329,639	40,992	10,688	40,654	14,301	0,280	<0,032
5	518111,944	9938013,737	6198,316	49,483	12,760	31,843	14,418	0,279	<0,032
6	516548,116	9938406,638	4976,450	54,670	17,834	35,630	12,753	0,253	<0,032
7	519043,762	9938142,561	5685,176	66,082	19,129	38,700	10,715	0,202	<0,032
8	516988,491	9938684,727	10534,623	504,572	9,936	21,184	32,487	0,260	<0,032
9	517291,677	9938540,281	9857,836	419,514	8,675	18,884	30,821	1, 276	<0,032
10	516518,068	9939047,484	12688,122	561,384	6,334	80,124	20,477	0,592	<0,032
11	516593,508	9938791,885	12621,349	256,812	9,627	81,204	16,494	0,581	<0,032
12	516964,523	9939178,332	9478,324	301,591	8,902	21,403	32,450	1,000	<0,032
13	516416,429	9939287,496	8538,727	404,236	9,768	18,285	22,983	1,155	<0,032
14	518150,360	9932125,964	10450,914	581,973	9,435	17,301	30,772	0,460	<0,032
15	518379,447	9932203,954	8034,677	423,818	9,905	19,190	29,654	0,255	<0,032
16	510918,800	9936976,460	10731,623	524,034	8,771	20,199	32,836	0,453	<0,032
17	520435,553	9955382,366	9054,631	349,926	9,001	21,800	28,059	0,347	<0,032
18	519353,172	9955860,297	10675,413	511,528	9,328	18,633	32,764	0,452	<0,032
19	519358,874	9955652,321	8012,036	424,077	9,004	20,883	29,488	0,259	<0,032
20	519178,533	9955583,536	9534,625	404,591	8,932	21,003	30,945	0,343	<0,032
21	519025,373	9955579,655	8084,094	519,264	9,327	16,773	29,035	0,269	<0,032
22	518748,143	9956004,597	10450,657	492,679	9,763	20,173	32,450	0,175	<0,032

Figure 7. Distribution of heavy metals contamination in paddy fields in Palaran Sub-district

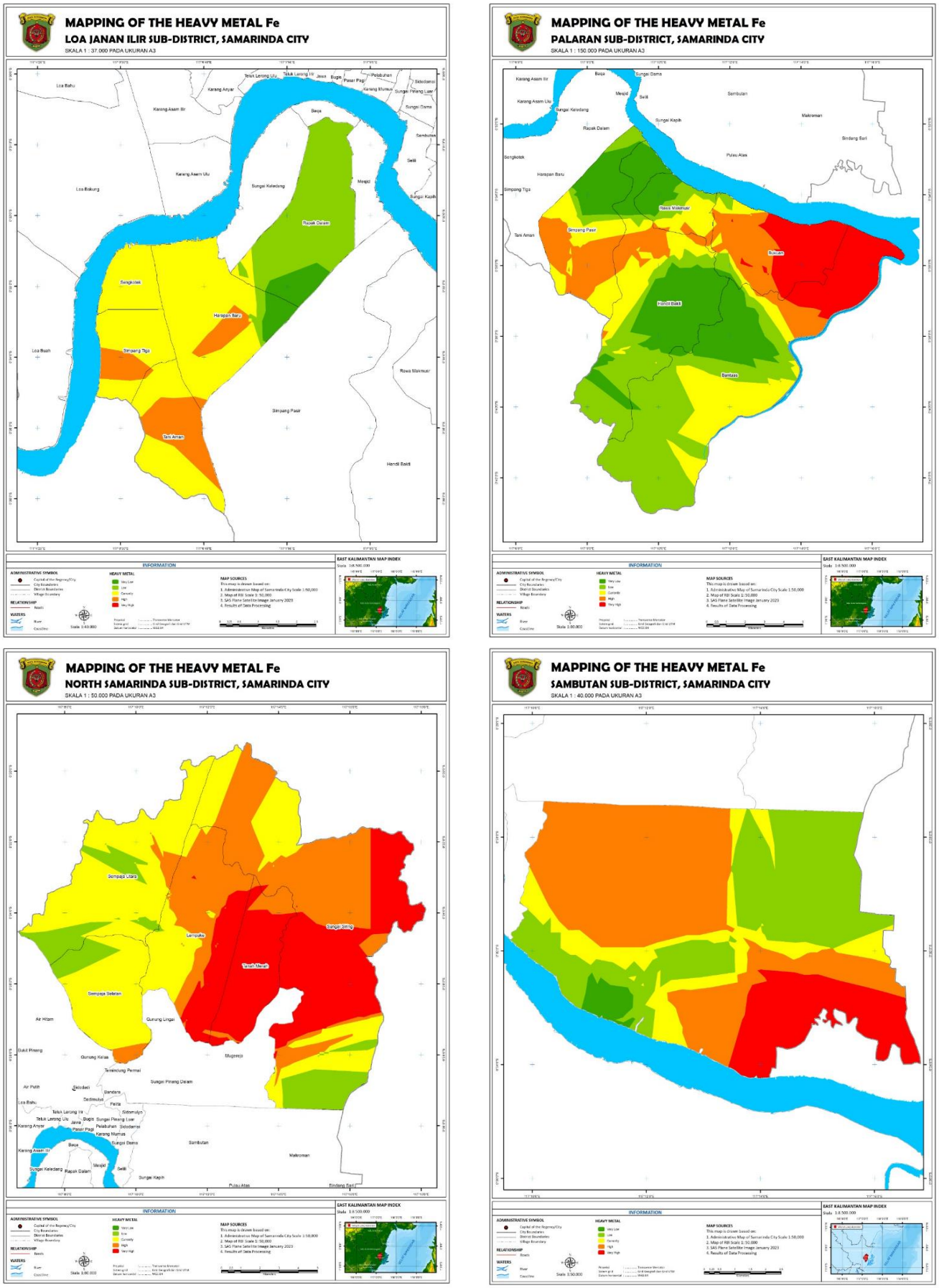

Figure 8. Mapping of the Fe distribution

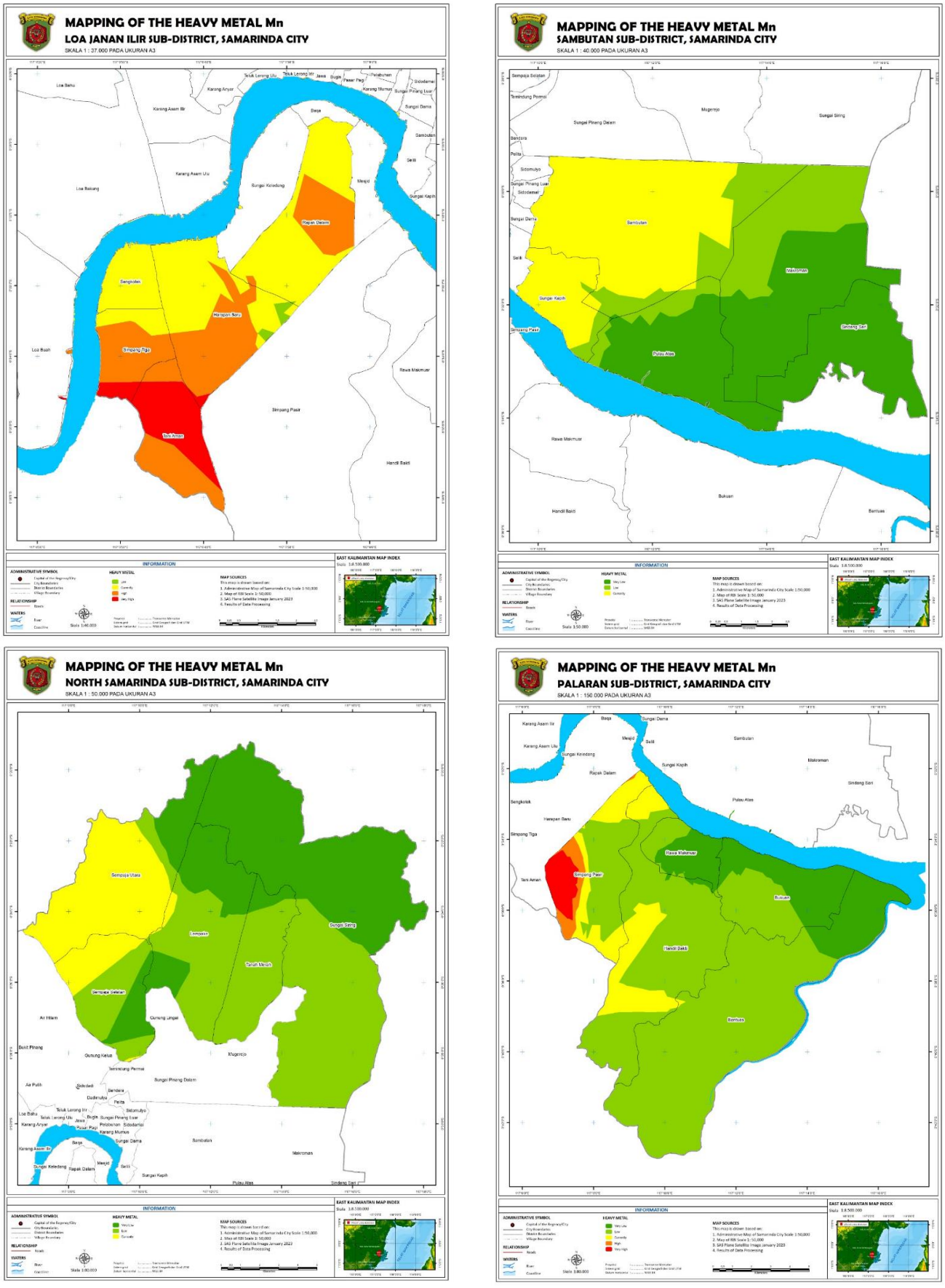

Figure 9. Mapping of the Mn distribution

Cd content in rice fields ranged from 0.04 ppm to 0.739 ppm, surpassing the critical Cd limit of 0.01 ppm according to SNI. The solubility of Cd increases in soil with a low pH (Lu et al. 2022), and cation exchange capacity (KTK) affects dissolved heavy metal concentrations (Cui et al. 2021). Organic matter from rice plants contributes to soil KTK, with higher KTK values indicating greater Cd tolerance (Gao et al. 2021). Cr content in rice fields in Samarinda was detected to be less than 0.032 ppm, categorized as very low based on the SNI threshold of 0.5 ppm. Chromium is a carcinogenic element released from industrial processes and poses risks even in small concentrations (Mitra et al. 2022). Chromium toxicity depends on its specifications, with hexavalent chromium [Cr(VI)] being more harmful than the trivalent form (Kapoor et al. 2022). Soil conditions influence the forms of chromium present, with Cr^{6+} being more mobile and toxic in oxidized conditions (Monga et al. 2022).

In conclusion, this study provides insights into the spatial distribution of heavy metal contamination in active rice fields in Samarinda. The findings indicate that Fe, Mn, Cu, Zn, Pb, and Cd concentrations in rice fields surpass critical limits established for soil, suggesting potential risks to agricultural and environmental health.

ACKNOWLEDGEMENTS

The authors are very grateful to the Soil Laboratory and Soil Cartography and GIS Laboratory Agriculture Faculty Universitas Mulawarman through the Doctoral Dissertation Analysis Research facilitating in 2023 for assisting with field spatial data collection.

REFERENCES

Abuzaid AS, Bassouny MA. 2020. Total and DTPA-extractable forms of potentially toxic metals in soils of rice fields, north Nile Delta of Egypt. Environ Technol Innov 18: 100717. DOI: 10.1016/j.eti.2020.100717.

Ahmed SF, Ullah H, Aung MZ, Tisarum R, Cha-Um S, Datta A. 2023. Iron toxicity tolerance of rice genotypes in relation to growth, yield and physiochemical characters. Rice Sci 30 (4): 321-334. DOI: 10.1016/j.rsci.2023.02.002

Akter R, Mukhles MB, Rahman MM, Rana MdR, Huda N, Ferdous J, Rahman F, Rafi MH, Biswas SK. 2022. Effect of pesticides on nitrification activity and its interaction with chemical fertilizer and manure in long-term paddy soils. Chemosphere 304: 135379. DOI: 10.1016/j.chemosphere.2022.135379.

Bashir S, Ali U, Shaaban M, Gulshan AB, Iqbal J, Khan S, Husain A, Ahmed N, Mehmood S, Kamran M, Hu H. 2020. Role of sepiolite for cadmium (Cd) polluted soil restoration and spinach growth in wastewater irrigated agricultural soil. J Environ Manage 258: 110020. DOI: 10.1016/j.jenvman.2019.110020.

Balai Penelitian Tanah. 2005. Petunjuk Teknis Analisis Kimia Tanah, Tanaman, Air, dan Pupuk. Balai Penelitian Tanah. Bogor. [Indonesian]

Bedoya-Perales NS, Maus D, Neimaier A, Escobedo-Pacheco E, Pumi G. 2023. Assessment of the variation of heavy metals and pesticide residues in native and modern potato (*Solanum tuberosum* L.) cultivars grown at different altitudes in a typical mining region in Peru. Toxicol Rep 11: 23-34. DOI: 10.1016/j.toxrep.2023.06.005.

Briat JF, Gojon A, Plassard C, Rouached H, Lemaire G. 2020. Reappraisal of the central role of soil nutrient availability in nutrient management in light of recent advances in plant nutrition at crop and molecular levels. Eur J Agron 116: 126069. DOI: 10.1016/j.eja.2020.126069.

BSN [Badan Standardisasi Nasional]. 2021. SNI-8910:2021. Cara uji kadar logam dalam contoh uji limbah padat, sedimen, dan tanah dengan metode destruksi asam menggunakan Spektrometer Serapan Atom (SSA)-Nyala atau Inductively Coupled Plasma Optical Emission Spectrometric (ICP-OES). www.bsn.go.id

Cakmak I, Brown P, Colmenero-Flores JM, Husted S, Kutman BY, Nikolic M, Rengel Z, Schmidt SB, Zhao F-J. 2023. Chapter 7 - Micronutrients. In: Rengel Z, Cakmak I, White PJ (eds). Marschner's Mineral Nutrition of Plants (4th Edition), Academic Press, Cambridge, Massachusetts. DOI: 10.1016/B978-0-12-819773-8.00017-4.

Cui X, Mao P, Sun S, Huang R, Fan Y, Li Y, Zhuang P, Li Z. 2021. Phytoremediation of cadmium contaminated soils by *Amaranthus hypochondriacus* L.: The effects of soil properties highlighting cation exchange capacity. Chemosphere 283: 131067. DOI: 10.1016/j.chemosphere.2021.131067.

Daulta R, Prakash M., Goyal S. 2023. Metal content in soils of Northern India and crop response: A review. Intl J Environ Sci Technol 20: 4521-4548. DOI: 10.1007/s13762-022-03953-y.

Diaconu M, Pavel LV, Hlihor RM, Rosca M, Fertu DI, Lenz M, Carvini PX, Gavrilescu M. 2020. Characterization of heavy metal toxicity in some plants and microorganisms-A preliminary approach for environmental bioremediation. New Biotechnol 56: 130-139. DOI: 10.1016/j.nbt.2020.01.003.

dos Santos MS, Sanglard LMVP, Barbosa ML, Namorato FA, de Melo DC, Franco WCG, et al. 2020. Silicon nutrition mitigates the negative impacts of iron toxicity on rice photosynthesis and grain yield. Ecotoxicol Environ Saf 189: 110008. DOI: 10.1016/j.ecoenv.2019.110008.

Dossou-Yovo ER, Kouadio SAK, Saito K. 2023. Effects of mid-season drainage on iron toxicity, rice yield, and water productivity in irrigated systems in the derived savannah agroecological zone of West Africa. Field Crops Res 296: 108901. DOI: 10.1016/j.fcr.2023.108901.

Gao J, Ye X, Wang X, Jiang Y, Li D, Ma Y, Sun B. 2021. Derivation and validation of thresholds of cadmium, chromium, lead, mercury and arsenic for safe rice production in paddy soil. Ecotoxicol Environ Saf 220: 112404. DOI: 10.1016/j.ecoenv.2021.112404.

Ha TV, Tuohy M, Irwin M, Tuan PV. 2020. Monitoring and mapping rural urbanization and land use changes using Landsat data in the northeast subtropical region of Vietnam. Egypt J Remote Sens Space Sci 23 (1): 11-19. DOI: 10.1016/j.ejrs.2018.07.001

Hembrom S, Singh B, Gupta SK, Nema AK. 2020. A comprehensive evaluation of heavy metal contamination in foodstuff and associated human health risk: A global perspective. In: Singh P, Singh R, Srivastava V (eds). Contemporary Environmental Issues and Challenges in Era of Climate Change. Springer, Singapore. DOI: 10.1007/978-981-32-9595-7_2.

Jaskulak M, Grobelak A, Vandenbulcke F. 2020. Modelling assisted phytoremediation of soils contaminated with heavy metals-Main opportunities, limitations, decision making and future prospects. Chemosphere 249: 126196. DOI: 10.1016/j.chemosphere.2020.126196.

Jiang Y, Chen S, Hu B, Zhou Y, Liang Z, Jia X, Huang M, Wei J, Shi Z. 2020. A comprehensive framework for assessing the impact of potential agricultural pollution on grain security and human health in economically developed areas. Environ Pollut 263: 114653. DOI: 10.1016/j.envpol.2020.114653.

Jiang Y, Hu T, Peng O, Chen A, Tie B, Shao J. 2021. Responses of microbial community and soil enzyme to heavy metal passivators in cadmium contaminated paddy soils: An in situ field experiment. Intl Biodeterior Biodegrad 164: 105292. DOI: 10.1016/j.ibiod.2021.105292.

Kapoor RT, Mfarrej MFB, Alam P, Rinklebe J, Ahmad P. 2022. Accumulation of chromium in plants and its repercussion in animals and humans. Environ Pollut 301: 119044. DOI: 10.1016/j.envpol.2022.119044.

Knuth F, Shean D, Bhushan S, Schwat E, Alexandrov O, McNeil C, Dehecq A, Florentine C, O'Neel S. 2023. Historical Structure from Motion (HSfM): Automated processing of historical aerial photographs for long-term topographic change analysis. Remote Sens Environ 285: 113379. DOI: 10.1016/j.rse.2022.113379.

Laurent C, Bravin MN, Crouzet O, Pelosi C, Tillard, Lecomte P, Lamy I. 2020. Increased soil pH and dissolved organic matter after a decade of organic fertilizer application mitigates copper and zinc availability despite contamination. Sci Tot Environ 709: 135927. DOI: 10.1016/j.scitotenv.2019.135927.

Li J, Huang X, Tu L, Zhang T, Wang L. 2022b. A review of building detection from very high resolution optical remote sensing images. GISci Remote Sens 59: 1199-1225. DOI: 10.1080/15481603.2022.2101727.

Li K, Wang J, Zhang Y. 2022a. Heavy metal pollution risk of cultivated land from industrial production in China: Spatial pattern and its enlightenment. Sci Total Environ 828: 154382. DOI: 10.1016/j.scitotenv.2022.154382.

Lu HL, Li KW, Nkoh JN, He X, Xu RK, Qian W, Shi R, Hong Z. 2022. Effects of pH variations caused by redox reactions and pH buffering capacity on Cd(II) speciation in paddy soils during submerging/draining alternation. Ecotoxicol Environ Saf 234: 113409. DOI: 10.1016/j.ecoenv.2022.113409.

Ministry of State for Population and Environment Republic of Indonesia and Dalhousie University Canada. 1992. Environmental Management in Indonesia. Report on Soil Quality Standards for Indonesia (interim report).

Mitra S, Chakraborty AJ, Tareq AM, Emran TB, Nainu F, Khusro A, Idris AM, Khandaker MU, Osman H, Alhumaydhi FA, Simal-Gandara. 2022. Impact of heavy metals on the environment and human health: Novel therapeutic insights to counter the toxicity. J King Saud Univ-Sci 34 (3): 101865. DOI: 10.1016/j.jksus.2022.101865.

Monga A, Fulke AB, Dasgupta D. 2022. Recent developments in essentiality of trivalent chromium and toxicity of hexavalent chromium: Implications on human health and remediation strategies. J Hazard Mater Adv 7: 100113. DOI: 10.1016/j.hazadv.2022.100113

Moreno-Lora A, Delgado A. 2020. Factors determining Zn availability and uptake by plants in soils developed under Mediterranean climate. Geoderma 376: 114509. DOI: 10.1016/j.geoderma.2020.114509.

Oprčkal P, Mladenovič A, Zupančič N, Ščančar J, Milačič R, Serjun VZ. 2020. Remediation of contaminated soil by red mud and paper ash. J Clean Prod 256: 120440. DOI: 10.1016/j.jclepro.2020.120440.

Otunola BO, Ololade OO. 2020. A review on the application of clay minerals as heavy metal adsorbents for remediation purposes. Environ Technol Innov 18: 100692. DOI: 10.1016/j.eti.2020.100692.

Palansooriya KN, Shaheen SM, Chen SS, Tsang DCW, Hashimoto Y, Hou D, Bolan NS, Rinklebe J, Ok YS. 2020. Soil amendments for immobilization of potentially toxic elements in contaminated soils: A critical review. Environ Intl 134: 105046. DOI: 10.1016/j.envint.2019.105046.

Qin G, Niu Z, Yu J, Li Z, Ma J, Xiang P. 2021. Soil heavy metal pollution and food safety in China: Effects, sources and removing technology. Chemosphere 267: 129205. DOI: 10.1016/j.chemosphere.2020.129205.

Rakotoson T, TsujimotoY, Nishigaki T. 2022. Phosphorus management strategies to increase lowland rice yields in sub-Saharan Africa: A review. Field Crops Res 275: 108370. DOI: 10.1016/j.fcr.2021.108370.

Sharma S, Kaur I, Nagpal AK. 2021. Contamination of rice crop with potentially toxic elements and associated human health risks-a review. Environ Sci Pollut Res 28: 12282-12299. DOI: 10.1007/s11356-020-11696-x.

Srivastav AL. 2020. Chapter 6 - Chemical fertilizers and pesticides: role in groundwater contamination. In: Prasad MNV (eds). Agrochemicals Detection, Treatment and Remediation: Pesticides and Chemical Fertilizers. Elsevier Ltd, Butterworth-Heinemann. DOI: 10.1016/B978-0-08-103017-2.00006-4.

Stefanowicz AM, Kapusta P, Zubek S, Stanek M, Woch MW. 2020. Soil organic matter prevails over heavy metal pollution and vegetation as a factor shaping soil microbial communities at historical Zn-Pb mining sites. Chemosphere 240: 124922. DOI: 10.1016/j.chemosphere.2019.124922 .

Steliga T, Kluk D. 2020. Application of Festuca arundinacea in phytoremediation of soils contaminated with Pb, Ni, Cd and petroleum hydrocarbons. Ecotoxicol Environ Saf 194: 110409. DOI: 10.1016/j.ecoenv.2020.110409 .

Tmušić G, Manfreda S, Aasen H et al. 2020. Current Practices in UAS-based Environmental Monitoring. Remote Sens 12 (6): 1001. DOI: 10.3390/rs12061001.

Wang J, Deng P, Wei X, Zhang X, Liu J, Huang Y, She J, Liu Y, Wan Y, Hu H, Zhong W, Chen D. 2023. Hidden risks from potentially toxic metal(loid)s in paddy soils-rice and source apportionment using lead isotopes: A case study from China. Sci Total Environ 856: 158883. DOI: 10.1016/j.scitotenv.2022.158883.

Wang Y, Duan X, Wang L. 2020. Spatial distribution and source analysis of heavy metals in soils influenced by industrial enterprise distribution: Case study in Jiangsu Province. Sci Tot Environ 710: 134953. DOI: 10.1016/j.scitotenv.2019.134953.

Wu P, Fu QL, Zhu XD, Liu C, Dang F, Müller K. 2020. Contrasting impacts of pH on the abiotic transformation of hydrochar-derived dissolved organic matter mediated by δ-MnO2. Geoderma 378: 114627. DOI: 10.1016/j.geoderma.2020.114627.

Zahoransky TE. 2022. Manganese speciation in soil studied by Mn K-edge X-ray absorption spectroscopy. [Dissertation]. Gottfried Wilhelm Leibniz Universität Hannover.

Zhang J, Liu Y, Sun Y, Wang H, Cao X, Li X. 2020. Effect of soil type on heavy metals removal in bioelectrochemical system. Bioelectrochem 136: 107596. DOI: 10.1016/j.bioelechem.2020.107596.

Zheng Q, Hou J, Hartley W, Ren L, Wang M, Tu S, Tan W. 2020. As (III) adsorption on Fe-Mn binary oxides: Are Fe and Mn oxides synergistic or antagonistic for arsenic removal?. Chem Eng J 389: 124470. DOI: 10.1016/j.cej.2020.124470.